

Numerical Simulation of Mixing and Combustion in Transient Sprays

T.Takagi, Y.Fukuyama*, T.Okamoto and Y.Nakano

*Department of Mechanical Engineering
Faculty of Engineering
Osaka University
Suita, Osaka 565
Japan*

* *Kubota Co. Ltd.*

ABSTRACT

Numerical simulations and analysis of transient sprays were made based on an Eulerian gas and a Lagrangian drop formulation coupled with a newly modeled chemical reaction procedure which takes into account intermediate species of H₂ and CO. The formulation consists of the conservation equations of mass, momentum, energy and species. All equations are solved numerically in fully coupled form. Numerical results are shown paying attention to the local mixing in the transient spray flame and parametric effects of injection velocity and ambient temperature on the combustion and soot formation.

INTRODUCTION

Spray combustion includes complex processes such as drop motion, evaporation as well as turbulent gaseous mixing and chemical reactions. Transient sprays with and without combustion as encountered in Diesel engines were experimentally studied in rapid compression machine⁽¹⁾ to get information about configuration and internal structure in the spray flames. Numerical simulations were made to simulate transient sprays with and without evaporation⁽²⁾. Computations of transient spray combustion⁽³⁾ were compared with experiments to verify the simulation method and to illustrate the ignition and the internal structure of the spray combustion.

The objectives of the present study are [1] to develop a combustion model taking into account intermediate species of H₂ and CO, [2] to predict local mixing rate in the combusting transient sprays which is related to the local heat release rate, and [3] to understand the effects of injection velocity and ambient temperature on the ignition delay, flame structure, mixing and soot concentration.

FUNDAMENTAL EQUATIONS

The fundamental equations are the transient Eulerian equations for the gas in cylindrical coordinates and the Lagrangian equations for the drops⁽²⁾. The equations include

[1] the conservation equations of mass, momentum and energy for the gas, [2] the conservation equations for gas species and soot, [3] the k- ϵ transport equations for turbulent kinetic energy and rate of turbulent energy dissipation, [4] the exchange rate equations of heat, mass and momentum between gas and drops⁽²⁾, [5] the state equation of the gas and [6] reaction models for gas species^{(4), (5), (6)} and soot^{(6), (7), (8)}.

Reaction models are the most indeterminable. In the present computations, three overall irreversible reactions are used to take intermediate species of H₂ and CO into account. The reaction model used in the present computation is shown in ref.(9). The validity of the model is verified by comparing with experiments on turbulent diffusion flames. The other equations are given in the references.^{(2),(3)} All equations are solved numerically in fully coupled form.

THE CONDITIONS AND THE METHOD OF COMPUTATIONS

The computed sprays are the axisymmetric transient ones that are formed when liquid fuel (tridecane) is injected from a single hole nozzle into stagnant, high-pressure and high-temperature air. An axisymmetric cylindrical volume is considered as the computation domain. The origin of the axisymmetric coordinate system is located at the center of the nozzle exit. The axial coordinate x is adjusted to the spray

Table 1 Spray conditions

Case	V _{inj}	T _{amb}	P _{amb}	Injection Duration
1	185 m/s	900 K	3 MPa	4 ms
2	185	900	3	2
3	365	900	3	2
4	555	900	3	2
5	365	950	3	2
6	365	1000	3	2

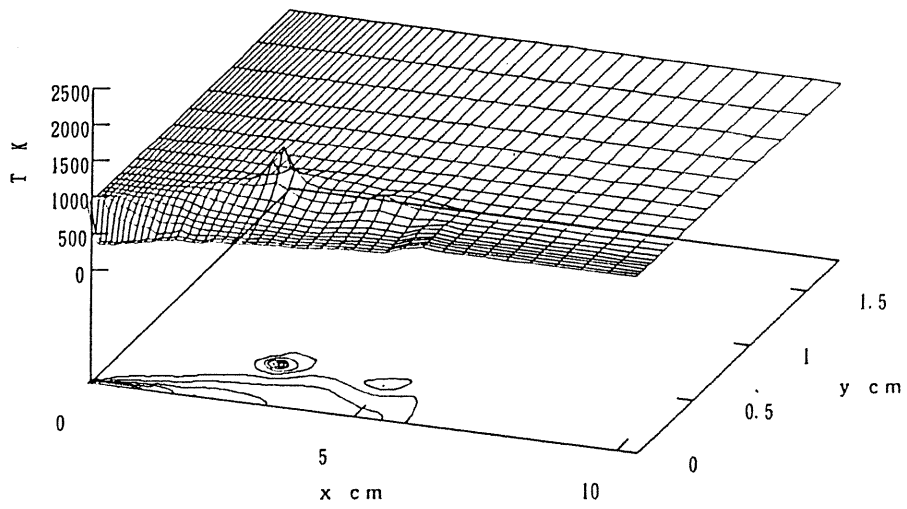
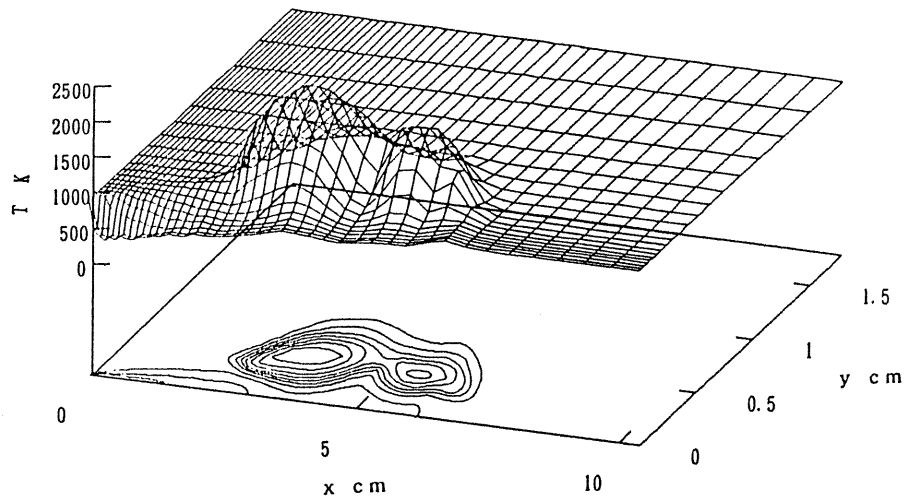
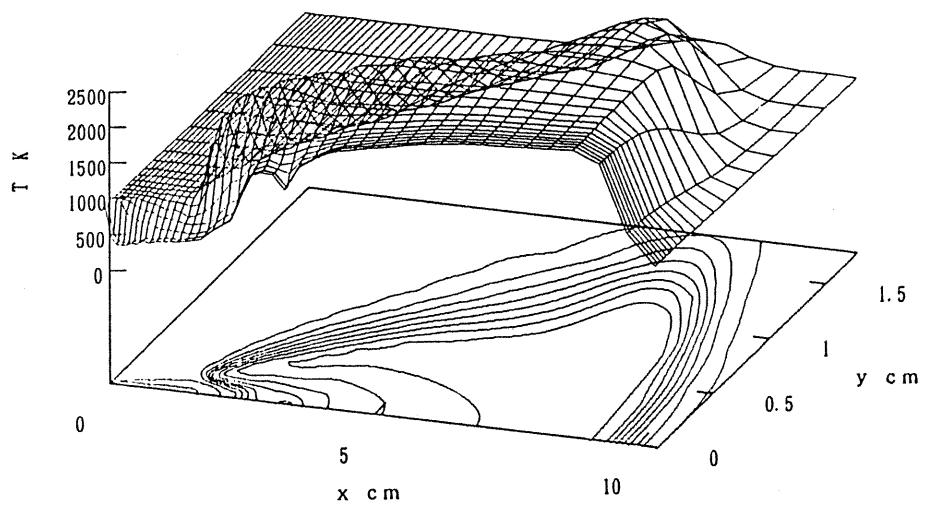
(a) $t = 1.0$ ms(b) $t = 1.3$ ms(c) $t = 4.0$ ms

Fig.1 Temperature profiles for the case 1

axis and the coordinate y is in the radial direction. The domain is divided into 44 cells in the x direction and 21 in the y direction.

The gas is stagnant initially. All dependent variables of the gas properties such as gas temperature, pressure, kinetic energy of turbulence, and its dissipation rate are assumed to be uniform initially. The downstream and side boundaries of the domain are treated as open boundaries where the radial and axial derivatives of the variables are set equal zero. The upstream boundary is treated as a solid wall with no slip for the velocity and zero normal gradients for scalar quantities. Drops are injected with injection velocity V_{inj} . The liquid

core at the nozzle exit is neglected. The drop size distribution at the nozzle exit is considered.

Table 1 shows the conditions of the calculations. The case 1 corresponds to that of experiments that was conducted with a rapid compression machine⁽¹⁾. The conditions of other cases are those for parametric studies of drop injection velocity and ambient temperature. P_{amb} and T_{amb} are the ambient pressure and temperature of the surrounding atmosphere. The drop mass-averaged radius at the exit of the nozzle is estimated from the injection velocity, gas density and surface tension⁽¹⁰⁾ for the case 1 and it was kept constant for all computation cases.

RESULTS AND DISCUSSIONS

Combustion and Mixing in a Typical Flame Case 1

Figure 1 shows the computed temperature profiles at different times t after the initiation of the fuel injection for the case 1. The profiles are in x - y plane which crosses the central axis. It indicates: (1) The minimum temperature is lower than the ambient temperature on the central part near the nozzle exit due to the heat absorption by the fuel drops. (2) The rapid temperature rise (ignition) initiates at about $t = 1$ ms and the location of the ignition (hot spot) is just upstream of the tip of the spray and off-axis region. (3) After ignition, the radial width of the spray increases due to the expansion of the gas. (4) Flame front is formed about 2 cm downstream from the nozzle exit.

Figure 2 shows the radial profiles of 7 species concentration (mole fraction) of fuel vapor, H_2O , CO_2 , O_2 , N_2 , H_2 , and CO , temperature T , mass fraction of soot Y_{SO} and local equivalence ratio ϕ at the cross section at $x=5.62$ cm and $t=4$ ms for the case 1. The radial profiles of species concentration and temperature are similar to those of gaseous turbulent diffusion flames⁽¹¹⁾. That is to say, the fuel vapor, CO and H_2 concentrations are high at the central part and

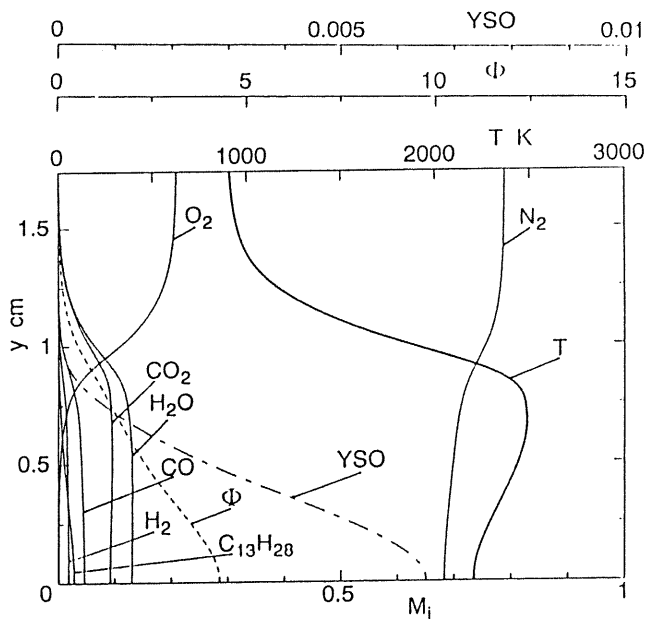


Fig.2 Radial profiles of concentration, temperature and equivalence ratio (case 1, $t = 4.0$ ms, $x = 5.62$ cm)

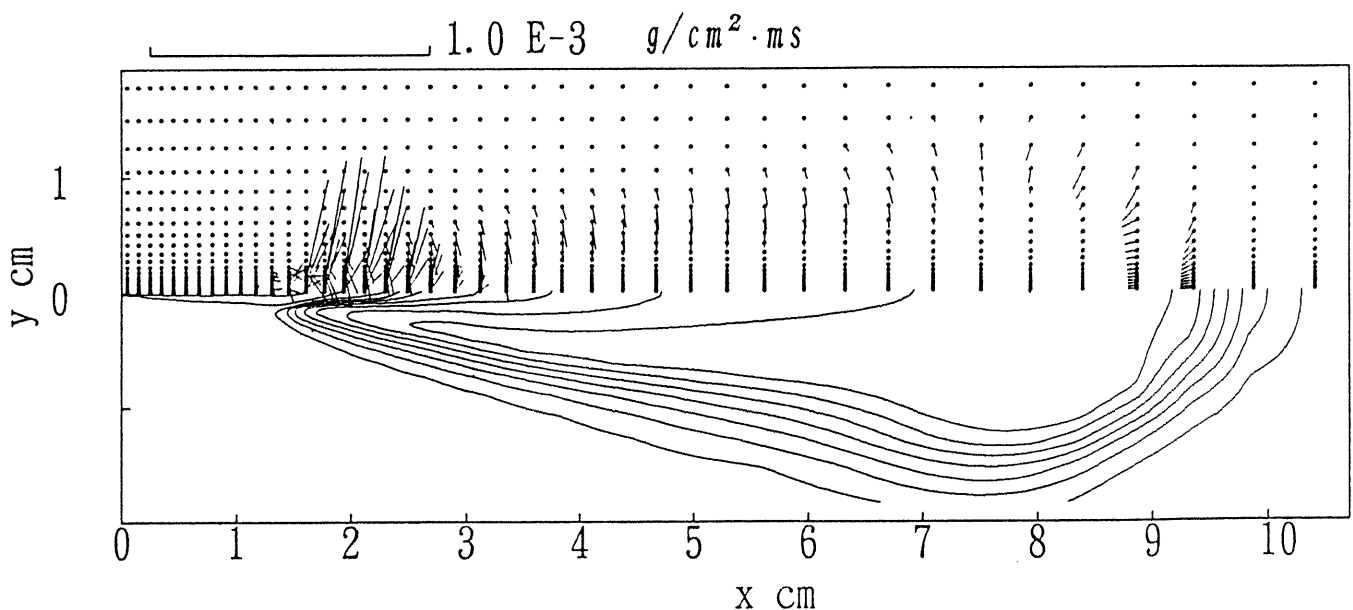


Fig.3 O_2 diffusion flux and corresponding temperature equi-contours (case 1, $t = 4$ ms)

O₂ is high at the outer part of the flame, respectively. CO₂ and H₂O concentration and temperature are high at the boundary where fuel vapor, H₂, CO and oxygen meet and equivalence ratio is about unity.

Figure 3 shows the local diffusion flux of O₂ at t=4 ms for the case 1, together with the equi-temperature contour. The magnitude and direction of the flux is shown by the vector in the Figure. The flux is evaluated by the concentration (mass fraction) gradient of O₂ multiplied by the turbulent effective diffusivity D_t and density at local points. The turbulent diffusivity is estimated from k-ε turbulence model. The diffusion flux which is relative to convection flux, should be the measure of the local intensity of mixing. It is noted: [1] the diffusion flux vector is toward the inner part of the flame at the tip and circumferential part, and [2] the mixing is most intense near the flame front at the upstream region where the local heat release rate is very intense⁽³⁾. Convection of O₂ is large in the upstream region near the central axis because O₂ is entrained by the spray without combustion near the nozzle exit. The entrained O₂ is diffused near the flame front.

Effects of Injection Velocity and Ambient Temperature

Figures 4 and 5 show heat release rate Q versus time t which is the total heat release rate due to reactions in the whole flow field for different conditions listed in Table 1. When the injection velocity increases, the peak of the heat release rate increases. The peak of the heat release rate just after the ignition comes from the premixed combustion where premixed mixture of fuel vapor and air burns. The higher peak of the heat release rate comes from the larger amount of premixed mixture of fuel vapor and air formed for higher injection velocity. The heat release rate decays faster for the case of higher injection velocity. This is because higher spray velocity promotes turbulent mixing and

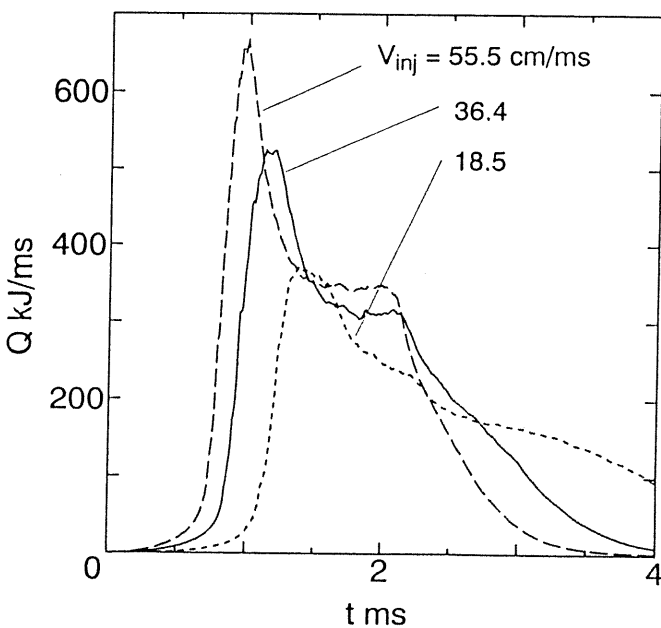


Fig.4 Total heat release rate versus time for the cases 2, 3 and 4

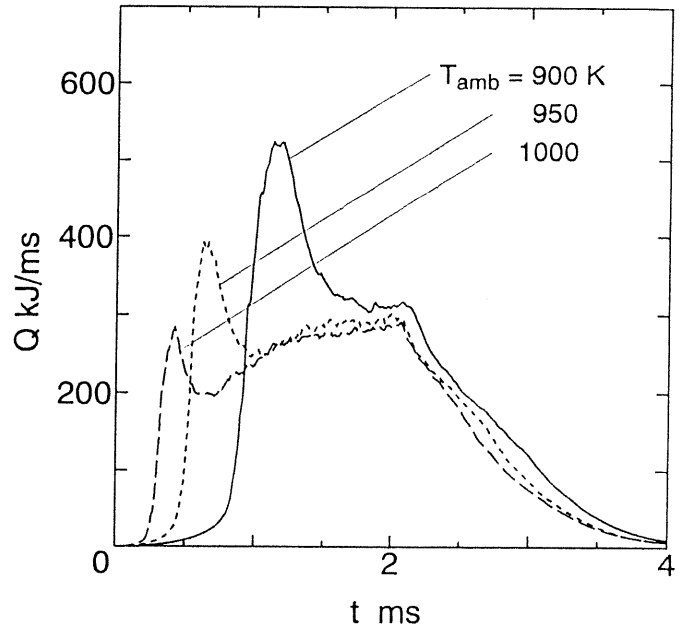


Fig.5 Total heat release rate versus time for the cases 3, 5 and 6

complete combustion.

Figure 5 shows the effect of ambient temperature on the heat release rate versus time. When the ambient temperature is higher, ignition delay decreases significantly and the peak of the heat release rate decreases. It indicates that the amount of the premixed mixture of fuel vapor and air formed prior to the ignition is smaller for the shorter ignition delay and so the premixed combustion is not intensive for short ignition delay. But the time needed for complete combustion is not so affected by the ambient temperature because the combustion of the final stage of the spray flame is dominated by the

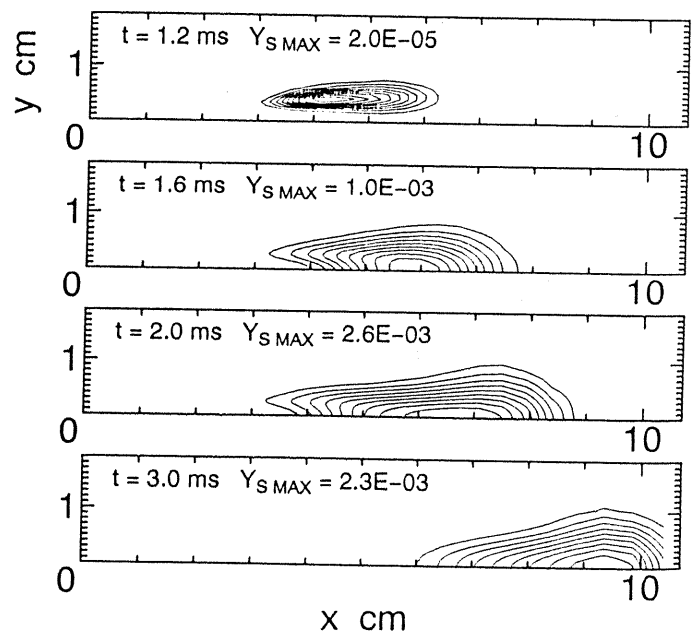


Fig.6 Equi-concentration of soot. (case 3)

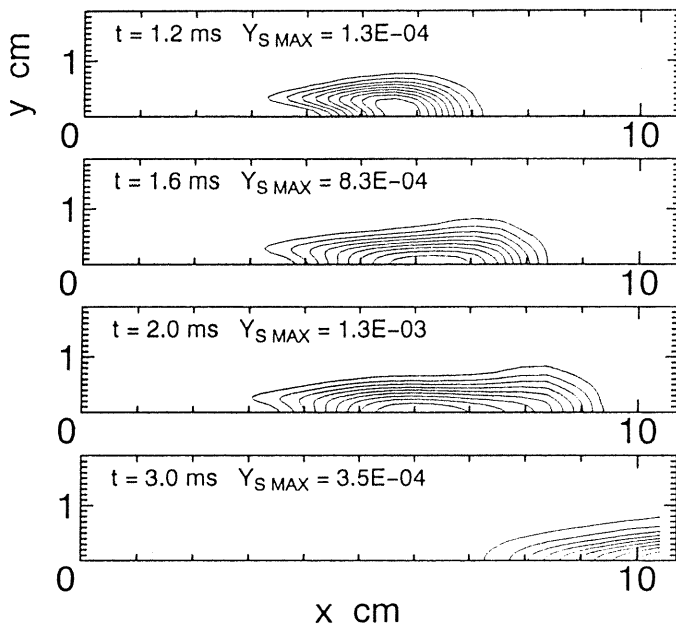


Fig.7 Equi-concentration of soot (case 4)

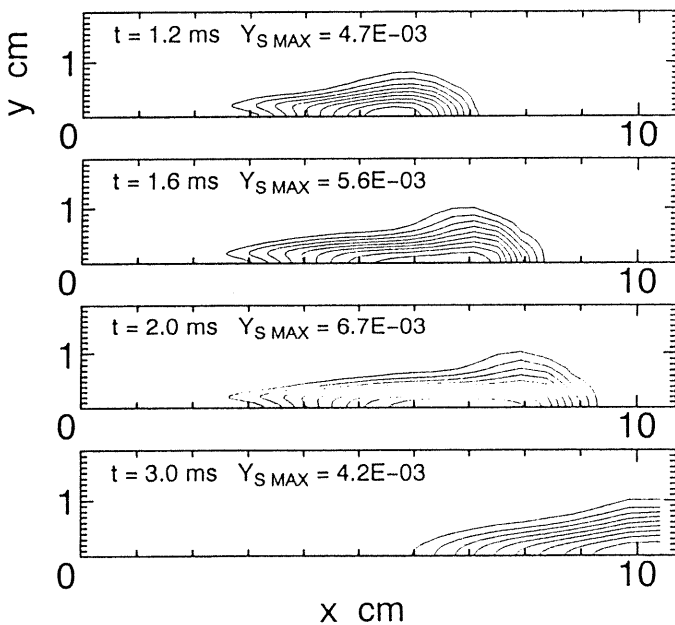


Fig.8 Equi-concentration of soot (case 5)

mixing speed rather than the speed of the chemical reactions.

Figures 6, 7 and 8 shows the equi-concentration lines of soot with respect to time for different injection velocity and ambient temperature. The soot concentration is evaluated in terms of the mass fraction of soot. The maximum value of the soot mass fraction, $Y_{S\text{ MAX}}$, is given in figures for respective time. Equi-concentration lines are drawn at regular intervals dividing the difference between the maximum and the minimum value into ten levels.

Comparison of Fig.6 (case 3) and 7 (case 4) indicates the effect of injection velocity. The injection velocity of fuel is

higher in case 4 than in case 3. The maximum soot mass fraction at $t = 1.2$ ms is higher in case 4 than in case 3. But, paying attention to the soot concentration found at $t = 1.6$ ms and after that time, it is noted that higher injection velocity results in lower maximum soot concentration $Y_{S\text{ MAX}}$.

Comparison of Fig.6 (case 3) and 8 (case 5) indicates the effect of ambient temperature. The ambient temperature is higher in case 5 than in case 3. It is noted that the maximum value of the soot fraction at respective time is higher in case 5 than that at same time in case 3. This suggests that the soot is liable to be formed much more for higher ambient temperature condition.

To analyze the factor leading to the change in soot formation corresponding to the change in the injection velocity and the ambient temperature, fuel mass fraction is calculated and its spatial distributions corresponding to Figs. 6, 7 and 8 is illustrated in Figs.9, 10 and 11. Here, we define the fuel mass fraction as the following formula.

$$Y_F = Y_{C_{13}H_{28}} + \frac{12}{44}Y_{CO_2} + \frac{12}{28}Y_{CO} + \frac{2}{18}Y_{H_2O} + Y_{H_2}$$

This value is equivalent to the mass fraction of the atoms which come from the fuel vapor, calculated with respect to only the gas phase, excluding the liquid phase. In addition, this value is considered as an index of mixing of the fuel vapor and the air and closely related to the soot formation.

Comparing Fig.9 (case 3) and Fig.10 (case 4), the maximum value of the fuel mass fraction is higher in case 3 than in case 4 at $t = 1.2$ ms. On the contrary, at $t = 1.6$ ms and after that time, that value is lower in case 4 than in case 3. This tendency coincides well with the behavior of the soot concentration found in Figs 6 and 7. Therefore, the reason why the higher injection velocity results in lower maximum

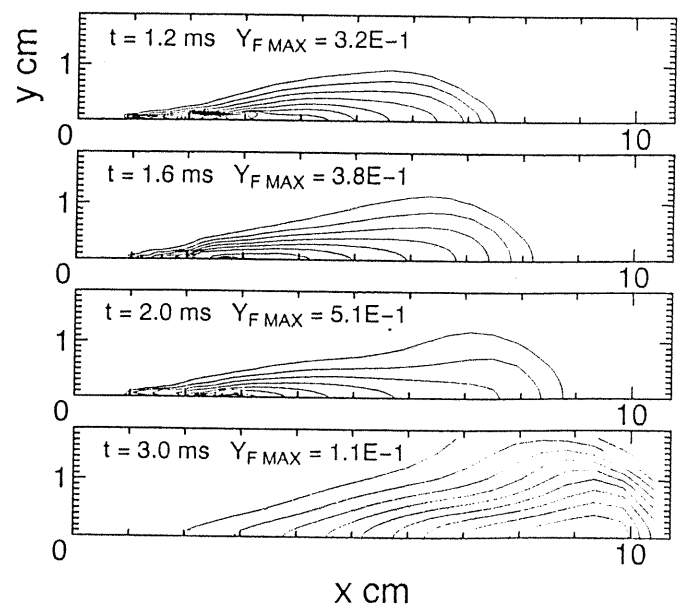


Fig.9 Distribution of fuel mass fraction (case 3)

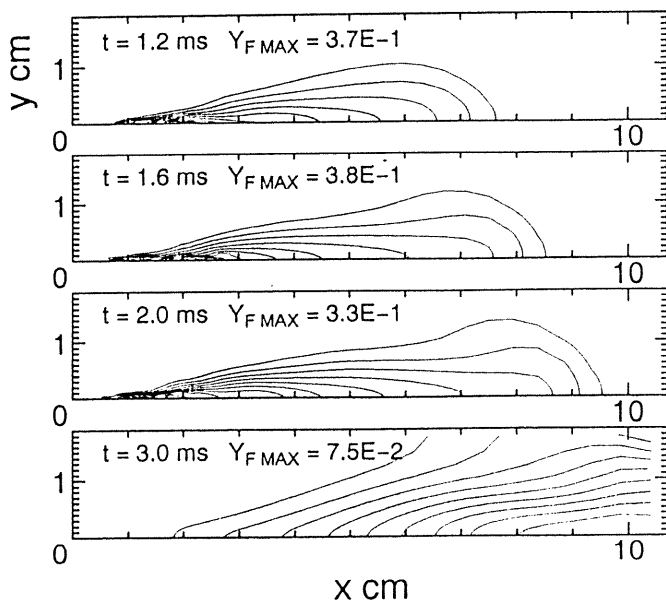


Fig.10 Distribution of fuel mass fraction (case 4)

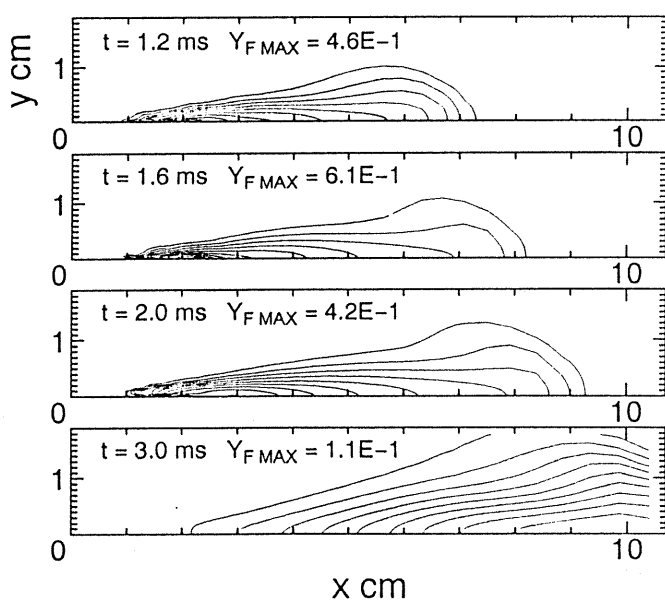


Fig.11 Distribution of fuel mass fraction (case 5)

soot concentration may be attributed to the fact that the mixing is enhanced due to higher injection velocity.

It is noticed, by comparing Figs. 9 and 11, that the maximum value of fuel mass fraction is always higher in case 5 than that at corresponding time in case 3. This comes from the higher evaporation rate due to higher ambient temperature. It is assumed easily that this higher fraction of fuel lead to higher soot formation rate in case 5 together with higher chemical reaction rate due to higher temperature.

SUMMARY

- (1) Three step reactions taking into account the intermediate species of H_2 and CO were incorporated for the numerical simulation of transient spray combustion.
- (2) A flame front appears downstream from the nozzle exit. Near the flame front, the diffusion of O_2 is very intense which corresponds to the intense local heat release rate. The entrainment of the air into the spray flow prior to the flame front results in the intense combustion at the flame front accompanied by the intense diffusion of O_2 .
- (3) High injection velocity results in rapid combustion and low soot formation accompanied by high mixing rate. High ambient temperature induces high soot formation due to the high chemical reaction rate and high mass fraction of fuel vapor.

REFERENCE

- (1) Yokota, H., Kamimoto, T. and Kobayashi, H., A Study of Diesel Spray and Flame by an Image Processing Technique (1st Rep.). Bulletin of JSME, 54, (1988), 741.
- (2) O'rourke, P. J. Collective Drop Effects on Liquid Spray, Ph. D. Thesis, (1981), Princeton University.
- (3) Takagi, T., Fang, C.Y., Kamimoto, T. and Okamoto, T., Comb. Sci. & Tech., 75, (1991),1.
- (4) Westbrook, C. K. and Dryer, F. L., Simplified Reaction Mechanisms for the Oxidation of Hydrocarbon. Combust. Scien. Techno., 27, (1981),31
- (5) Aggarwal, S. K.(1987). Chemical-Kinetics Modeling for the Ignition of Idealized Sprays. Combust. Flame, 69, 291.
- (6) Magnussen, B. F. and Hjertager, B. H.(1977). On Mathematical Modeling of Turbulent Combustion With Special Emphasis on Soot Formation and Combustion. Sixteenth Symposium (International) on Combustion, p.719, The Combustion Institute.
- (7) Lee, K. B., Thring, M. W. and Beer, J. M.(1962). On the Rate of Combustion of Soot in a Laminar Soot Flame. Combust. Flame, 6, 137.
- Lefebvre, A.H.(1989). Atomization and Sprays, Hemisphere Publishing Corporation, New York.
- (8) Abbas, A. S. and Lockwood, F. C.(1985). Prediction of Soot Concentrations in Turbulent Diffusion Flames. J. Inst. Energy., September,112.
- (9) Fukuyama, Y., Takagi, T. and Okamoto, T., Numerical Analysis of Transient Spray Combustion, 30th Combustion Symposium (Japan), (1992), 319.
- (10) Kuo, T. W. and Bracco, F. V.(1982). Computations of Drops Sizes in Pulsating Sprays and of Liquid-Core Length in Vaporizing Sprays. SAE paper, 820133.
- (11) Takagi, T., Okamoto, T.(1986). Fundamental Studies on the Structure of Turbulent Diffusion Flames (3rd Report). Bulletin of JSME., 52, 1540.